ELSEVIER

Journal of Photochemistry and Photobiology A: Chemistry 124 (1999) 127–133

Journal of Photochemistry and Photobiology A:Chemistry

Photophysical properties: laser activity of and energy transfer from 1,4-bis[β-(2-benzothiazolyl)vinyl]benzene (BVB)

Samy A. El-Daly

Department of Chemistry, Faculty of Science, Tanta University, Tanta, Egypt

Received 24 November 1998; accepted 22 March 1999

Abstract

The photophysical properties such as singlet absorption, molar absorptivity, fluorescence spectra and fluorescence quantum yield of BVB have been measured in different solvents as well as in micelles and microemulsion media. Both electronic absorption and fluorescence spectra are sensitive to medium acidity and in acidic media the fluorescence maximum is obtained at 500 nm. The quantum yields for photochemical transformation (ϕ_c) of BVB have been determined in different organic solvents at room temperature. The laser activity of BVB has also been investigated. Dye solution in DMF gives laser emission around 460 nm upon excitation by 337.1 nm nitrogen laser pulse. BVB acts as a good energy donor for *N*,*N*′-bis(2,6-dimethylphenyl)-3,4:9,l0-perylenebis(dicarboximide) (DXP). The energy transfer obeys Förster type mechanism. © 1999 Elsevier Science S.A. All rights reserved.

Keywords: l,4-Bis[β-(benzothiazolyl)vinyl]benzene; Laser dyes; Medium effect; Energy transfer

1. Introduction

Diolefinic compounds containing heterocyclic moieties of the general formula Ar′–CH=CH–Ar–CH=CH–Ar′ have been extensively reported as laser dyes of reasonable photostability [1–8]. Other applications are in UV stabilization of polymers [9], electrochromic display and optical imaging devices [10,11] and electroluminescent devices [12]. A new candidate in this family of compounds is 1,4-bis[β-(2-benzothiazolyl)vinyl]benzene (BVB). In the present paper we report the spectral characteristics and photostability and laser action of this compound as well as excitation energy transfer to *N*,*N*′-bis(2,6-dimethylphenyl)-3,4:9,10-perylenebis(dicarboximide) (DXP).

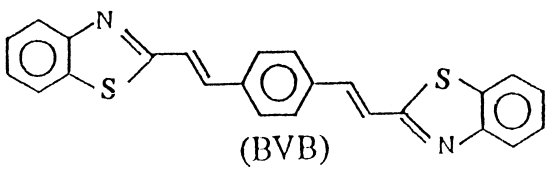

(BVB)

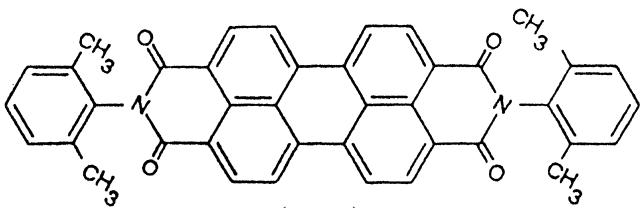

(D×P)

2. Experimental

l,4-Bis[β-(2-benzothiazolyl)vinyl] benzene was prepared according to the general condensation procedure reported for the preparation of this series of diolefinic compounds [13]. The dye was recrystallized twice from dimethylformamide (DMF). The material was then vacuum sublimed in the dark. *N*,*N*′-bis(2,6-dimethylphenyl)-3,4:9,10-perylenebis-(dicarboximide) (Aldrich) was purified by vacuum sublimation. Cetyltrimethyl ammonium chloride (CTAC, Kodak) was used to prepare cationic micelles. Microemulsion solutions were prepared using chloroform (oil), water, sodium dodecyl sulfate (SDS) surfactant and butanol (co-surfactant). Water in oil (w/o) microemulsions were prepared by mixing these components in ratio (by weight) 37.075:4.308:4.308:4.306, respectively, and oil in water (o/w) microemulsions by mixing them in the ratio 2.06:43.62:2.06:2.06, respectively [14]. Hammett's acidity scale (H_0) [15] was followed in preparing solution of pH<1.0. All solvents used in the measurements were of spectroscopic grade.

Steady-state fluorescence together with fluorescence and photochemical quantum yields were measured using Shimadzu RF-510 spectrofluorophotometer with band-pass of 10 nm using right-angle arrangement. The fluorescence spectra were corrected for the machine response using 10^{-5} mol dm^{-3} anthracene solution in benzene as reported

1010-6030/99/$ – see front matter
PII: S1010-6030(99)00069-6

earlier by Melhuish [16]. UV–visible absorption spectra were recorded on Shimadzu UV-160 A spectrophotometer with band-pass of 5 nm. Fluorescence quantum yields (ϕ_f) were measured relative to either 9,10-diphenyl anthracene or quinine sulfate [17,18] according to the wavelength range of emission. Low sample concentrations ($\leq$0.1 absorbance units) were used to avoid reabsorption.

The following relation has been applied to calculate the fluorescence quantum yields.

$$\phi_f(s) = \phi_f(r) \frac{\int I_s(\bar{v})d\bar{v}}{\int I_r(\bar{v})d\bar{v}} \times \frac{A_r}{A_s} \times \frac{n_s^2}{n_r^2}.$$

The integrals represent the corrected fluorescence peak areas, A is the absorbance at the excitation wavelength, and n is the refractive index of the solvent used. The subscript 's' and 'r' refer to sample and reference, respectively. Light intensity was measured by using ferrioxalate actinometry [19]. Photochemical quantum yields (ϕ_c) have been measured using a method that accounts for the decrease in absorbance at the excitation wavelength as the photoreaction proceeds as described previously [1].

The lasing action of the dye was monitored in a dye laser (GL-302 Dye Laser, PTI) pumped by a nitrogen laser (GL-3300 Nitrogen Laser, PTI), the pump laser (λ_{ex}=337.1 nm) was operated at repetition of 3 Hz with a pulse energy of 1.48 mJ and pulse duration of 800 Ps. The narrow-band output of the dye laser was measured with a pyroelectric Joulemeter (ED 100, Gen-Tec). The energy of the pump laser was measured with a second pyroelectric Joulemeter (ED 200, Gen-Tec).

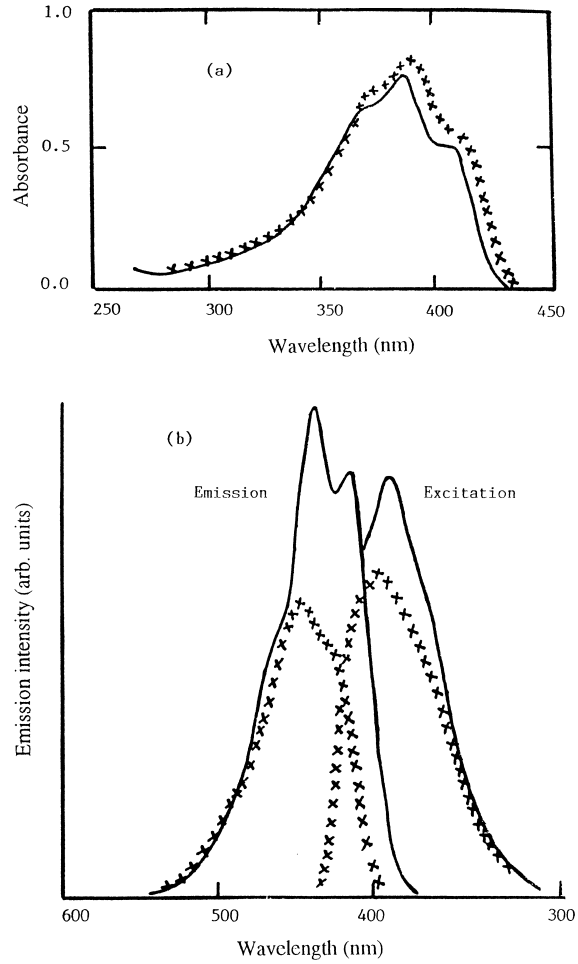

Fig. 1. (a) Electronic absorption spectra of 1×10^{-5} M of BVB solution in (———) *n*-heptane and in (××××) MeOH. (b) Emission and excitation spectra of 1×10^{-5} in (———) *n*-heptane and in (×××) MeOH (λ_{ex}=392 nm).

3. Results and discussion

3.1. Effect of medium on the spectral characteristics

The electronic absorption, excitation and emission spectra of BVB were measured in 14 different solvents of different polarities (Δf). Fig. 1 shows the electronic absorption, emission and excitation spectra of BVB of two solvents of different polarities, namely *n*-heptane and methanol. The solvent polarity shows a slight effect on the position of the electronic absorption maxima. The small shifts in the position of the absorption spectra indicate a little change in dipole moments on going from ground state to excited state. As the solvent polarity (Δf) increases, the emission spectra become red-shifted. The absorption and fluorescence maxima of BVB are red shifted by 6 and l4 nm on going from *n*-heptane to methanol, respectively. There is also a good mirror image relationship between absorption and fluorescence spectra and a coincidence between absorption and excitation maxima. These facts together with the high molar absorptivities are consistent with a strongly allowed transition with a small geometry change between electronic ground and excited state. In non-polar solvents, however, e.g. *n*-heptane fluorescence spectra exhibit more fine structures compared with polar-protic solvents e.g. methanol as shown in Fig. 1(b). This could be due to specific solvent–solute interaction. The Franck–Condon peak occurs at the second vibrational peak in electronic absorption and emission spectra and also no effect of excitation energy on the position of emission maximum which indicated that the different conformers of BVB have the same energy or only one conformer is present. The spectral data of BVB are presented in Table 1. The fluorescence quantum yields (ϕ_f) of BVB are much affected by the solvent polarity (Δf). As shown in Table 1, the values of ϕ_f decreases with increasing solvent polarity. This could be attributed to efficient internal conversion and/or intersystem crossing by extensive mixing between the close-lying $^1(\pi,\pi^*)$ and $^1(n,\pi^*)$ states. In addition non-radiative rate increases markedly in solvents with strong hydrogen bonding character and competes with fluorescence emission [20,21].

The emission and excitation spectra of BVB in micro-emulsion media have also been studied. Fig. 2 shows both the emission and excitation spectra in chloroform, w/o and

Table 1
Spectral behavior and fluorescence quantum yield (ϕ_f) of BVB in different solvents

Solvent	$\Delta f(D,n)$	ϵ_{max} l mol^{-1} cm^{-1}	λ_{ab}(max) (nm)	λ_{ex}(max) (nm)	λ_{em}(max) (nm)	ϕ_f
n-Heptane	0.001	76600	386	387	436	0.86
Carbon tetrachloride	0.0117	57700	396	388	443	0.66
Dioxane	0.020	57800	390	394	445	0.75
Toulene	0.029	57710	390	394	445	0.63
Ether	0.167	57500	392	394	446	0.56
Chloroform	0.149	56800	392	395	446	0.51
n-Butanol	0.246	54600	392	395	450	0.48
n-Propanol	0.280	54700	392	395	450	0.48
Cyclohexanol	0.299	49800	392	395	450	0.45
Methanol	0.309	48300	392	395	450	0.25
Ethylene glycol	0.276	–	394	396	450	0.18
Dimethyl formamide	0.274	54500	392	396	450	0.48
Acetone	0.287	52300	390	393	450	0.38
Acetonitrile	0.305	52500	393	395	450	0.45

o/w microemulsions. In o/w microemulsions the spectral pattern is red shifted compared with the emission spectra in w/o microemulsions. Both emission and excitation spectra of BVB in w/o microemulsions resemble that in pure chloroform (λ_{em}(max)=446 nm, λ_{ex}(max)=396 nm). Fluorescence quantum yields of BVB have been measured in w/o and o/w microemulsions. A ϕ_f value of (0.54) in w/o is higher than that in o/w microemulsions (ϕ_f=0.12). The ϕ_f value in w/o is nearly equal to that measured in chloroform (ϕ_f=0.51), whereas the ϕ_f value in o/w is lower than that in bulk chloroform or in w/o microemulsions. This due to high solubility of BVB in chloroform. The low values of ϕ_f in the o/w system is presumably due to hydrogen bond formation with dominant water molecules.

BVB is insoluble in water but undergoes solubilization in cationic micelle e.g. CTAC, with subsequent increase in fluorescence intensity. An abrupt increase in fluorescence intensity is observed at surfactant concentration corresponding to the critical micelle concentration (cmc) [22,23] as shown in Fig. 3. The structured spectra of BVB in CTAC above cmc indicate that the BVB molecules are located in the non-polar hydrocarbon core of micelles.

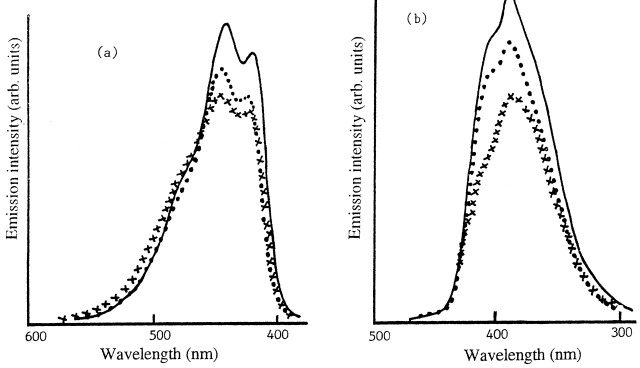

Fig. 2. (a) Emission spectra of 1×10^{-6} M of BVB in (———) $CHCl_3$, (···) w/o and (×××) o/w microemulsions (λ_{ex}=392 nm). (b) Excitation spectra of 1×10^{-5} M BVB in (———) $CHCl_3$, (···) w/o and (××××) o/w microemulsions. Excitation spectra were measured by following the emission maxima.

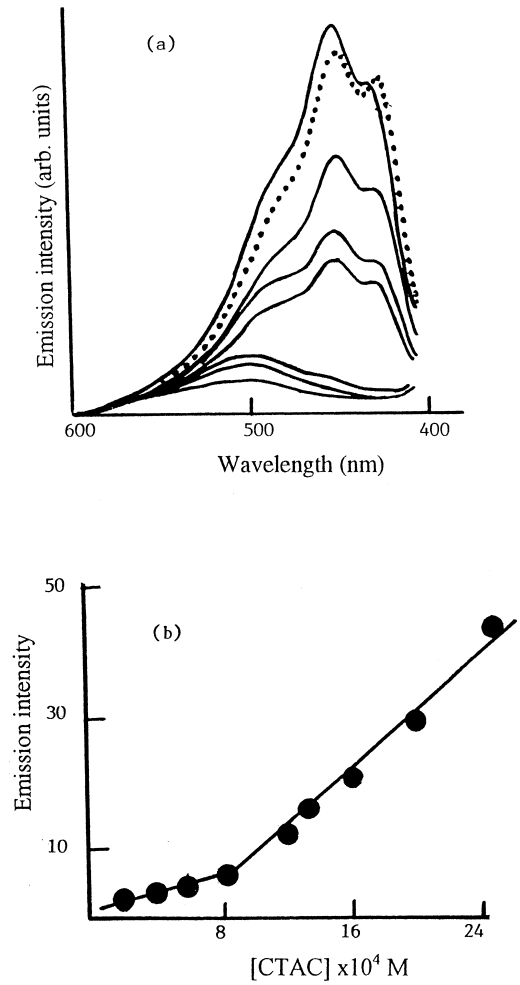

Fig. 3. (a) Emission spectra of 1×10^{-6} M of BVB in different concentrations of CTAC. The concentrations of CTAC at increasing emission intensities are: 2×10^{-4}, 4×10^{-4}, 6×10^{-4}, 8×10^{-4}, 10×10^{-4}, 12×10^{-4}, 14×10^{-4} and (···) 1×10^{-2} M (λ_{ex}=392 nm). (b) Plot of emission intensity at emission maximum against CTAC concentrations.

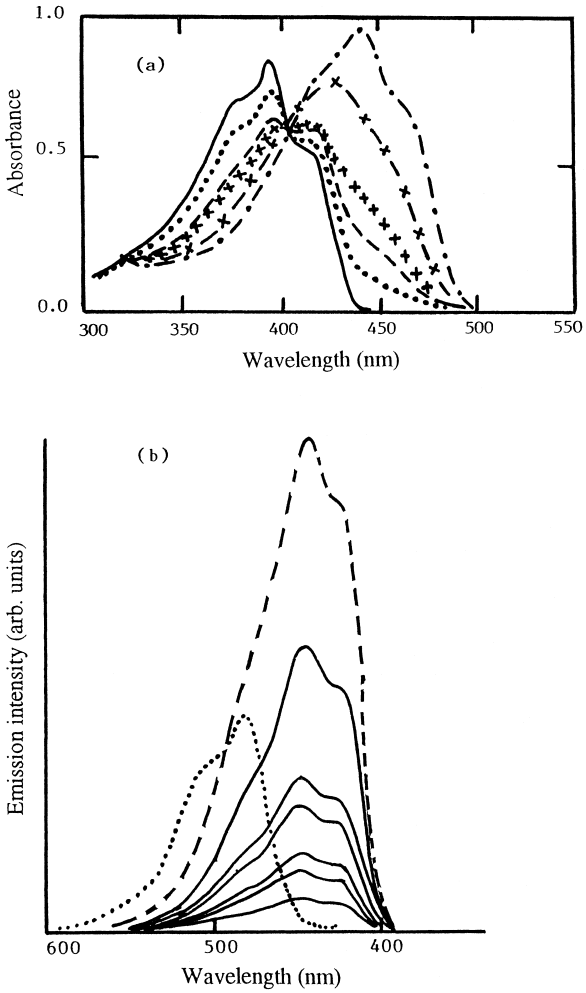

Fig. 4. (a) Electronic absorption spectra of 1×10^{-5} M of BVB in (———) DMF and in different values of H_0. The values of H_0 at decreasing absorbance at 392 nm are: 0.9, 0.7, 0.5, 0.4 and 0.22. (b) Emission spectra of 1×10^{-5} of BVB in (- - -) DMF and in different values of H_0. The values of H_0 at decreasing emission intensity at 450 nm are 0.9, 0.7, 0.5, 0.4. 0.12 (λ_{ex}=392 nm). The dotted spectrum is the emission spectrum of BVB at H_0=0.18 (λ_{ex}=420 nm).

The effect of medium acidity on the electronic absorption and fluorescence spectra has been studied. The electronic absorption and emission spectra of BVB in DMF were measured at different hydrogen ion concentrations (H_0). In acidic media a new absorption band develops at 423 nm with an isobestic point at ca. 406 nm as shown in Fig. 4. The fluorescence spectral pattern also changes in acidic media upon increasing medium acidity, the emission at 450 nm decreases in intensity. The change in both absorption and emission spectra of BVB in acidic media is obviously due to protonation of heterocyclic nitrogens with subsequent development of the spectral pattern. The protonation constant of ground state (pk) was determined by UV-spectrophotometric and fluorometric titration according to half-height method. Both absorbance-pH and fluorescence intensity-pH curves display the same value of pk as 0.55. This indicates that the lifetimes of respective prototropic species are shorter than the reciprocal rate constant for the protonation and deprotonation reactions. The excited state protonation constant pk^* were calculated by using the following relation [24]:

$$pk - pk^* = 2.10 \times 10^{-3}(\bar{\nu}_{BH^+} - \bar{\nu}_B).$$

The quantities $\bar{\nu}_{BH^+}$ and $\bar{\nu}_B$ represent the wavenumber of pure electronic transition in acidic and conjugate base, respectively. The wave numbers were obtained from electronic absorption spectra giving pk^* values termed pk^*_{ab} wavenumber obtained from fluorescence spectra give pk^* values termed pk^*_f. For BVB in DMF, $pk^*_{ab} = 3.8$ and $pk^*_f = 3.46$. The values of pk^* are consistent with the earlier observation that the tertiary nitrogen atom becomes more basic on excitation to s_1 state. There is a small difference between the pk^* values obtained by using absorption and fluorescence maxima. This is because, the solvent relaxation for the respective species are nearly the same in the ground and excited states.

3.2. Photostability of BVB

Photostability of BVB has been studied in different organic solvents. Fig. 5 shows the effect of photoirradiation (λ_{ex}=392, I_0=6.1×10^{-6} Ein min^{-1} on the electronic absorption spectra of 1×10^{-5} M of BVB in methanol and dimethylformamide. Photoirradiation using 392 nm light causes a decrease in the absorbance at 392 nm and a photostationary state is reached upon prolonged irradiation. The original absorption spectrum, on the other hand is regenerated almost quantitatively upon irradiation of the photoproduct using short wavelength light of λ=337 nm. At such low concentration of diolefinic dyes, the dominant photoreaction is believed to be a *trans-cis* photoisomerization process. This view is substantiated by the attainment of a photostationary state and the back reaction on using 337 nm light. The photochemical quantum yield (ϕ_c) values of BVB in different solvents are summarized in Table 2. The low values of ϕ_c and back photochemical reaction induced by 337 nm light can make BVB a good laser dye.

Table 2
Photochemical quantum yield (ϕ_c) of BVB in different solvents (λ_{ex}=392, I_0=6.1×10^{-6} Ein min^{-1})

Solvent	ϕ_c
Dioxane	0.023
Carbon tetrachloride	0.017
Chloroform	0.012
n-Propanol	0.14
Methanol	0.16
Dimethyl formamide	0.013
Acetonitrile	0.015

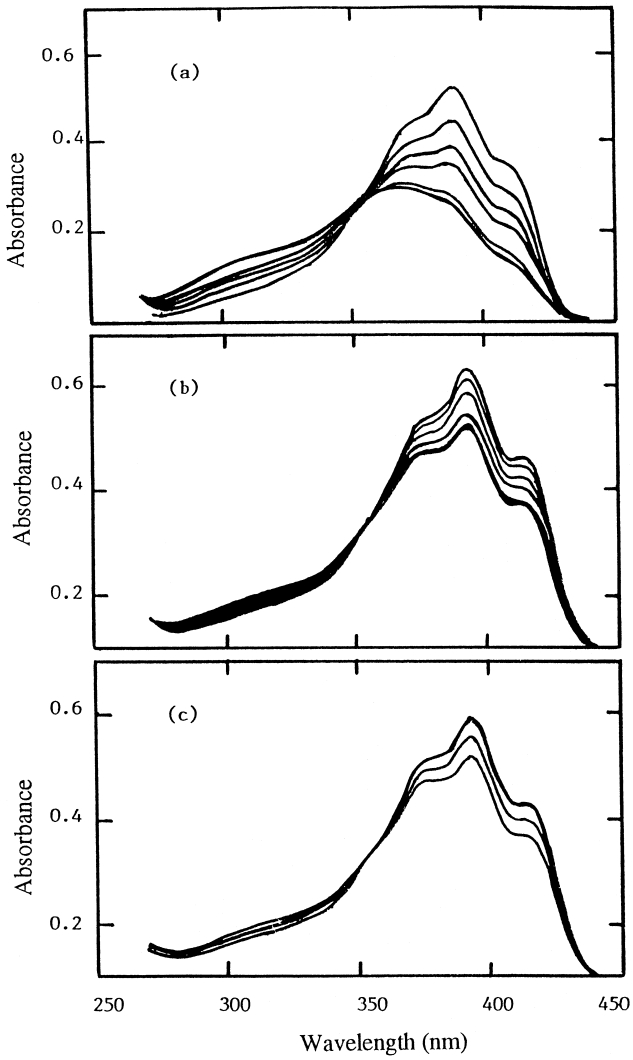

Fig. 5. Effect of photoirradiation (λ_{ex}=392 nm) on absorption spectrum (a) in MeOH; (b) in DMF. The irradiation times for decreasing absorbance are 0, 1, 2, 3, 8, 12, 22 and 70 min for MeOH and 0, 2, 5, 10, 20, 30 and 55 for DMF. (c) The back photoreaction induced by using short wavelength light (λ_{ex}=337 nm) in irradiating the photoproduct. The irradiation times at increasing absorbance are: 0, 20 and 30 min.

3.3. Laser activity of BVB

2×10^{-3} M solution of BVB in DMF was excited by nitrogen laser pulses (λ_{ex}=337.1 nm) of 800 Ps duration with 1.48 mJ. The dye solution was taken in oscillator and amplifier cuvettes of 1 cm path length. Output of laser dye was measured by power meter as a function of wavelength to determine the lasing range. BVB gives laser emission in the wavelength range 430–480 nm with emission maximum at 460 nm of 0.18 mJ energy per pulse. The gain coefficient $\alpha(\lambda)$ of laser emission of BVB was calculated by measuring the intensity I_L of laser emission from the entire cell length L and the intensity $I_{L/2}$ from the cell half-length, one can evaluate the laser gain $\alpha(\lambda)$ [25] from the following relation:

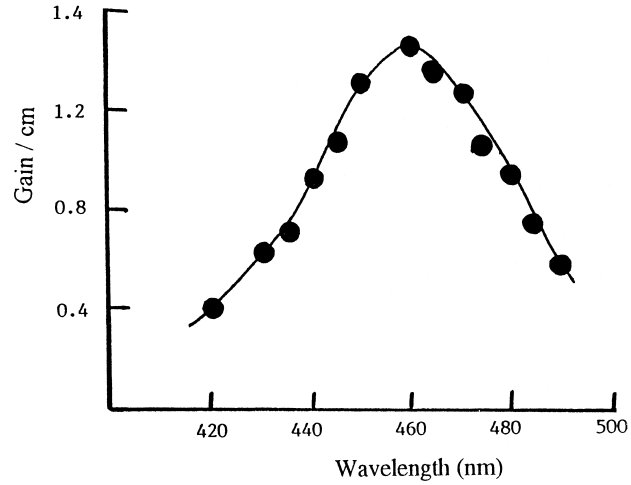

Fig. 6. Gain spectrum of laser emission from 2×10^{-3} M of BVB in DMF.

$$\alpha(\lambda) = \frac{2}{L}\ln\left[\frac{I_L}{I_{L/2}} - 1\right].$$

The gain spectrum of BVB is shown in Fig. 6. The cross-section for stimulated laser dye emission σ_e was calculated at laser emission maximum (λ=460 nm) according to the equation [26]

$$\sigma_e = \frac{\lambda_e^4 E(\lambda)\phi_f}{8\pi c_0 n^2 \tau_f},$$

where λ_e is the emission wavelength, n the refractive index of the solution, c the velocity of light and $E(\lambda)$ is the normalized fluorescence line-shape function. For BVB dye value of $\sigma_e=1.76\times10^{-16}$ cm^2 was obtained at 460 nm which is close to the values for best laser dyes [26]. BVB dye acts as a good energy donor for laser dyes, which have low molar absorptivities at 337 nm such as DXP. A mixture of BVB and DXP laser dyes give laser emission tail of the fluorescence spectrum of the acceptor in the emission range 540–610 nm with emission maximum at 580 nm upon excitation by nitrogen laser pulses (λ_{ex}=337.1 nm). This establishes the fact that lasing takes place in acceptor only. Thus most of the excitation energy absorbed by the donor is transferred to the acceptor as a useful pump power making excitation transfer efficient. Fig. 7(a) shows the output energy of maximum laser emission (λ=580 nm) of DXP in DMF as solvent in presence of different concentrations of BVB (donor). For increase in the concentration of the donor, self-absorption is responsible for screening the tunable laser action. Thus the maximum output energy of laser decreases with increasing the concentration of BVB in the dye mixture. In addition to the above ETDL study, fluorescence energy transfer characteristics have also been studied to determine the rate constant of energy transfer and also ascertain the nature of energy transfer involved in the BVB/DXP system. The rate constant (k_{ET}) of energy transfer in BVB/DXP system in DMF

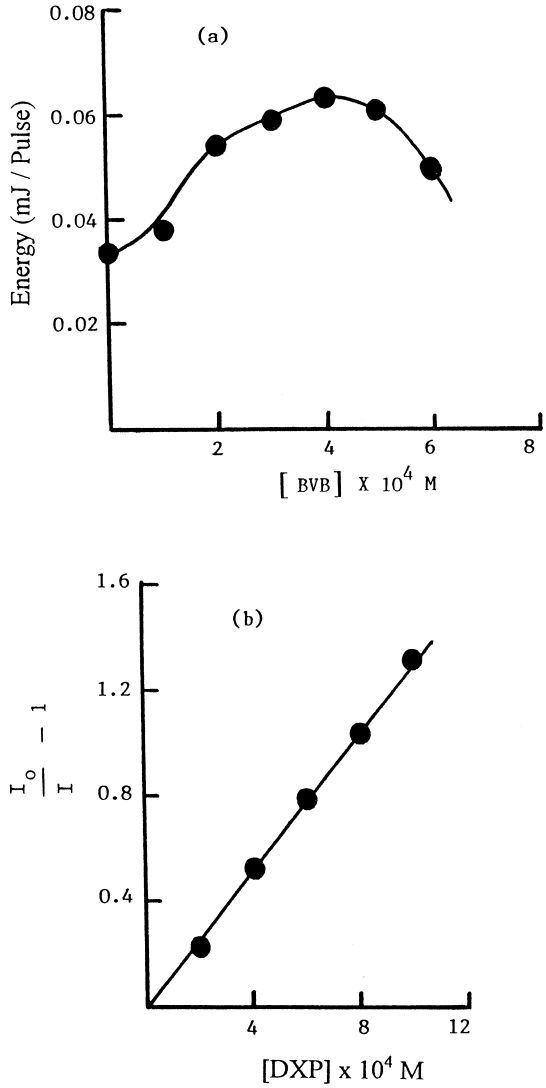

Fig. 7. (a) Output energy of laser emission of 1×10^{-3} M DXP against the concentration of BVB (λ_{em}=580 nm). (b) Stern–Volmer plot of fluorescence quenching of 1×10^{-5} M BVB by DXP (λ_{ex}=337 nm, λ_{em}=450 nm).

was calculated from the fluorescence quenching study by using 0.2 cm cuvette. Fig. 7(b) shows the Stern–Volmer plot of BVB fluorescence quenching using DXP as a quencher by applying the Stern–Volmer relation in the form [27].

$$\frac{I_0}{I} = 1 + k_{ET}\tau[Q],$$

where I_0 and I are fluorescence intensities in the absence and the presence of the quencher of concentration [Q] in M, the rate constant of energy transfer k_{ET} in $M^{-1}s^{-1}$ and τ is the solution lifetime taken as 0.9 ns in DMF. From the slope of Fig. 7(b), k_{ET} has been calculated as $k_{ET}=1.12\times10^{12}$ $M^{-1}s^{-1}$. This value is much higher than the diffusion-controlled rate constant (k_{diff}) in DMF at room temperature. From the spectral data shown in Fig. 8, it is seen that there is a significant overlap between the electronic absorption of

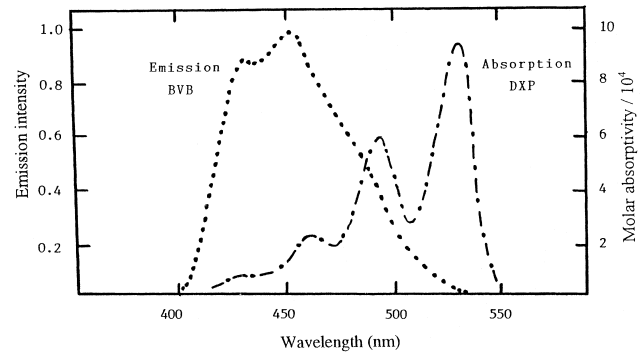

Fig. 8. Emission spectrum (λ_{ex}=337 nm) of 1×10^{-5} M BVB dye in DMF (···) and absorption spectrum of 1×10^{-5} M DXP in DMF (– · –).

DXP and the emission of BVB. Applying Förester's resonance energy transfer mechanism, the critical transfer distance R_0 has been calculated for BVB/DXP system using the following relation [28]:

$$R_0^6 = \frac{1.25\times10^{-25}\times\phi_f}{n^4}\int_0^\infty \frac{F_D(\bar{\upsilon})\epsilon_A(\bar{\upsilon})}{(\bar{\upsilon})^4}d\bar{\upsilon},$$

where R_0 is the distance at which energy transfer and emission processes are equally probable, ϕ_f is the emission quantum yield of donor in the absence of acceptor, n is the refractive index of the solvent, and the integral is the overlap integral for fluorescence spectrum of donor normalized to unity (F_D) and the absorption spectrum of acceptor (ϵ_A) divided by the fourth power of wave number $\bar{\nu}$. The critical transfer distance (R_0) was found as R_0=49.5 Å. This value is higher than that for collosional energy transfer in which R_0 values are in the range of 4 – 6 Å [29]. The high value of critical transfer distance as well as quenching rate constant indicate that the underlying mechanism of energy transfer is that of resonance energy transfer due to dipole–dipole interaction between excited donor $(BVB)^*$ and ground state acceptor (DXP).

4. Conclusion

The following conclusion can be arrived to from the above studies. BVB dye has high fluorescence quantum yield, high molar absorptivity at 337 nm and high photostability when excited at 392 nm and back photochemical reaction upon excitation at 337 nm. These properties make BVB a good laser dye. The dye gives strong laser emission at 460 nm. BVB dye acts as good energy donor for laser dyes which have low molar absorptivities at 337 nm.

Acknowledgements

We thank Prof. S. Hirayama of Kyoto Institute of Technology for lifetime measurements of BVB sample.

References

[1] S.A. EI-DaIy, S.M. Al-Hazmy, E.M. Ebeid, A.C. Bhasikuttan, D.K. Palit, A.V. Saper, J.P. Mittal, J. Phys. Chem. 100 (1996) 9732.
[2] S.A. EJ-Daly, S.M. Al-Hazmy, E.M. Ebeid, B.M. Vernigor, J. Photochem. Photobiol. A 91 (1995) 199.
[3] E.M. Ebeid, M.M.F. Sabry, S.A. El-Daly, Laser Chem. 5 (1985) 223.
[4] M. Hasegawa, H. Harashia, T. Hosokawa, Jpn. Kakai Tokyo Koho JaP. Patent 89 (1989) 57618.
[5] M. Nohara, M. Hasegawa, C. Hosokawa, H. Tokallin, T. Kusumoto, Chem. Lett. 2 (1990) 189.
[6] S. Yongjia, R. Shengwu, Dyes Pigments 15 (1991) 157, 183.
[7] E.M. Ebeid, R.M. Issa, S.A. El-Daly, M.M.F. Sabry, J. Chem. Soc., Faraday Thans. 2(82) (1986) 1981.
[8] S.A. El-Daly, E.M. Ebeid, S.M. Al-Hazmy, A.S. Babaqi, Z. El-Gohary, G. Duportial, Proc. Indian Acad. Sci. 105 (1993) 651.
[9] G. Irick, C.A. Kelly, J.C. Martin, US Patent 4 075 162 (1978); G. Irick, Jr., C.A. Kelly, US Patent 4 096 115 (1978).
[10] A. Hirohashi, K. Akutagawa, M. Sumiya, Y. Ito, Jpn. KoKai Tokyo Koho (1988).
[11] A.I. Bykh, V.M. Golovenko, N.N. Rozhitskii, Deposited Doe. SPSTL 1114 Khp-D82, 1982.
[12] C. Hosokawa, T. Kusumoto, H. Tokailin, H. Higashi, Eur. Patent Appl. (1990).
[13] B.M. Venigor, V.K. Shalaev, L.P. Novaseltseva, V.F. Zakharov, Khim. Geterotsikl Soedin 5 (1980) 604.
[14] E.M. Ebeid, M.H. Abdel-Kader, R.M. Issa, S.A. El-Daly, Chem. Phys. Lett 146 (1988) 331.
[15] M.J. Jorgenson, D.R. Hatter, J. Am. Chem. Soc. 79 (1957) 427.
[16] W.H. Melhuish, J. Phys. Chem. 64 (1960) 762.
[17] J.V. Morris, M.A. Mahaney, J.R. Huber, J. Phys. Chem. 80 (1976) 969.
[18] J.N. Demas, G.A. Crosby, J. Phys. Chem. 75 (1971) 991.
[19] I.G. Hatchard, C.A. Parker, Proc. Roy. Soc. London, Ser. A 235, 518 (1959).
[20] S.C. Shim, M.S. Kim, K.T. Lee, B.H. Lee, J. Photochem. Photobiol. A 67 (1992) 23.
[21] T.D.Z. Atvars, C.A. Bortolato, D. Dibbern Brunelli, J. Photobiol. A 68 (1991) 41.
[22] H.F. Eicke, Top. Curr. Chem. 87 (1980) 1, 86.
[23] C.A. Bunton, Prog. Sol. State Chem. 8 (1973) 239.
[24] B. Marciniak, H. Kozubek, Pasyc, J. Chem. Educ. 69(3) (1992) 247.
[25] P. Chou, D. McMorrow, T.J. Aatsma, M. Kasha, J. Phys. Chem. 88 (1984) 4596.
[26] M. Rink, H. Gusten, H.J. Ache, Phys. Chem. 90 (1986) 2661.
[27] G.R. Penzer, in: S.B. Brown (Ed.), An Introduction to Spectroscopy for Biochemists, Academic Press, London, 1980, p. 86.
[28] A. Gilbert, J. Baggott, Essentials of Molecular Photochemistry, Blackwell, London, 1991, p. 186.
[29] S.G. Schulman, in: E.L. Wehry (Ed.), Modern Fluorescence Spectroscopy, vol. 2, Plenum Press, New York, 1976.